Three-dimensional Structure of FEZ-1, a Monomeric Subclass B3 Metallo-β-lactamase from Fluoribacter gormanii, in Native Form and in Complex with d-Captopril

I Garcıa-Sáez, P S Mercuri, Cyril Papamicaël, R Kahn, J M Frère, M Galleni, G M Rossolini, O Dideberg

doi:10.1016/S0022-2836(02)01271-8 *J. Mol. Biol.* (2003) **325**, 651–660

JMB

Available online at www.sciencedirect.com

SCIENCE DIRECT®

Three-dimensional Structure of FEZ-1, a Monomeric Subclass B3 Metallo-β-lactamase from *Fluoribacter gormanii*, in Native Form and in Complex with D-Captopril

I. García-Sáez[1], P. S. Mercuri[2], C. Papamicael[3], R. Kahn[1], J. M. Frère[2] M. Galleni[2], G. M. Rossolini[4] and O. Dideberg[1]*

[1]*Institut de Biologie Structurale (CIP), Jean-Pierre Ebel (CNRS-CEA), 41, rue Jules Horowitz, 38027 Grenoble Cedex 1, France*

[2]*Université de Liège Institut de Chimie Laboratoire d'Enzymologie, B6 Sart-Tilman, B-4000 Liège Belgium*

[3]*Oxford Center for Molecular Sciences, South Parks Road Oxford OX1 3QY, UK*

[4]*Dipartimento di Biologia Molecolare, Sezione di Microbiologia, Università degli Studi di Siena, Policlinico La Scotte, I-53100 Siena, Italy*

**Corresponding author*

The β-lactamases are involved in bacterial resistance to penicillin and related compounds. Members of the metallo-enzyme class are now found in many pathogenic bacteria and are thus becoming of major clinical importance. The structures of the Zn-β-lactamase from *Fluoribacter gormanii* (FEZ-1) in the native and in the complex form are reported here. FEZ-1 is a monomeric enzyme, which possesses two zinc-binding sites. These structures are discussed in comparison with those of the tetrameric L1 enzyme produced by *Stenotrophomonas maltophilia*. From this analysis, amino acids involved in the oligomerization of L1 are clearly identified. Despite the similarity in fold, the active site of FEZ-1 was found to be significantly different. Two residues, which were previously implicated in function, are not present in L1 or in FEZ-1. The broad-spectrum substrate profile of Zn-β-lactamases arises from the rather wide active-site cleft, where various β-lactam compounds can be accommodated.

Keywords: antibiotic resistance; binuclear zinc; crystal structure; oligomer; Zn-β-lactamase

Introduction

The Zn-β-lactamases provide a powerful and threatening weapon that renders bacteria resistant to antibiotics. Powerful, because they have a broad-range of activity against different substrates (e.g. penicillins, cephalosporins) and particularly against third-generation penicillins (carbapenems[1]), which are hydrolyzed poorly by most of the serine-β-lactamases. Threatening because no clinically efficient inhibitor has been characterized. Moreover, the appearance of Zn-β-lactamases encoded by mobile elements, such as the IMP-type and VIM-type enzymes[2,3] has promoted the spread of similar enzymes to major bacterial pathogens, such as Enterobacteriaceae, *Pseudomonas aeruginosa*, and other Gram-negative species.[4] Due to these particularities, the biochemical and structural characterization of members of the increasingly large family of Zn-β-lactamases are of great interest, since a detailed analysis of the active site and mechanism of action of these enzymes could lead to rational design of inhibitors, which could be co-administrated with β-lactam antibiotics.

The Zn-β-lactamases (Ambler class B β-lactamases) are characterized by the presence of one or two metal-binding sites in their active site.[5,6] Interestingly, a specific enzyme may utilize either one or both zinc ions for maximal activity. Consequently, they are inhibited by chelating agents such as EDTA, 1,10-*o*-phenanthroline and dipicolinic acid.[7] Despite the high degree of overall

Abbreviation used: ESRF, European Synchrotron Radiation Facility.

E-mail address of the corresponding author: otto@ibs.fr

0022-2836/03/$ - see front matter

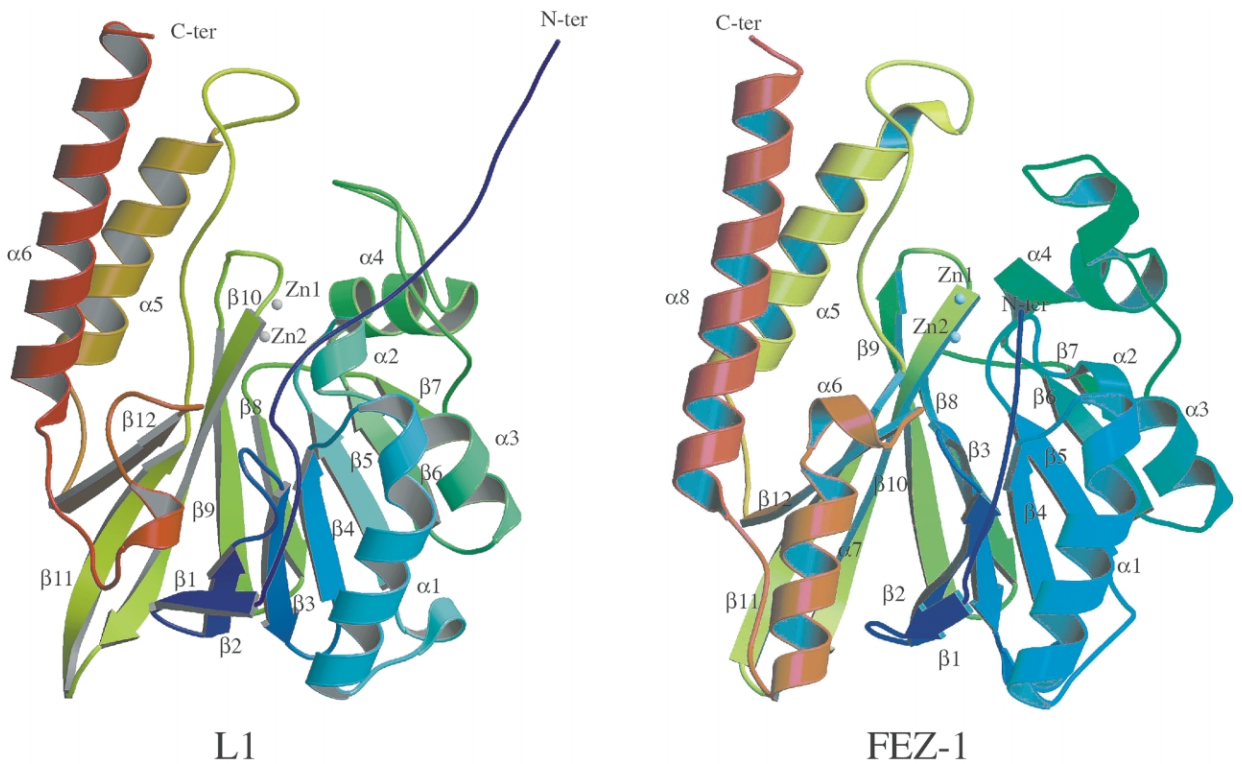

Figure 1. Structural comparison between FEZ-1 and L1 monomer; both structures are represented as ribbons. Secondary structures are labeled and the backbone is colored in a rainbow ramp. The two zinc ions are shown as blue spheres. The 3D representation was made using MOLSCRIPT.[28]

structural similarity between the different Zn-β-lactamase structures obtained to date,[8,9] there are differences that have been used to cluster class B β-lactamases into three different subclasses: B1, B2 and B3.[10] Subclass B1 contains the first studied and better known Zn-β-lactamases (e.g. BcII from *Bacillus cereus*, CcrA or CfiA from *Bacteroides fragilis*, IMP-1 from *P. aeruginosa* and *Serratia marcescens*). They are monomers and are active with one or two Zn ions in their active sites. In contrast, the subclass B2 Aeromonas enzymes (CphA, ImiS and CphA2) are inhibited by the presence of the second Zn ion in the active site. Finally, subclass B3 includes the tetrameric enzyme L1 from the opportunistic pathogen *Strenotrophomonas maltophilia*, GOB-1 from *Chryseobacterium meningosepticum*, THIN-B from *Janthinobacterium lividum*, FEZ-1 from *Fluoribacter gormanii*[11,12] and Mbl1b from *Caulobacter crescentus*.[13]

Like L1 and GOB-1, FEZ-1 exhibits a broad-spectrum activity profile, with a strong preference for cephalosporins such as cephalothin, cefuroxime and cefotaxime; in contrast to the tetrameric L1, it has been shown to be monomeric in solution.[12]

Here, we present the three-dimensional structures of the native form of FEZ-1 and of the complex with the inhibitor D-captopril at 1.65 Å and 1.78 Å resolution, respectively. These structures are compared with that of the tetrameric member of the subclass B3, L1.

Results

Overall structure

Two different crystal forms for FEZ-1 were obtained at two different pH values (5.0 and 7.0) without and with D-captopril in the crystallization droplet. The native crystals are monoclinic $P2_1$ with two molecules per asymmetric unit, whereas the crystals obtained in presence of D-captopril are monoclinic C2 with one molecule per asymmetric unit. The overall structure of FEZ-1 in both crystal forms (262 residues from 36–311 following BBL numbering[10]) conserves the main structural features of class B β-lactamases[8] and particularly those found in L1.[14] The structure folds as a αβ/βα sandwich, where the helices are exposed to the solvent and surround the compact core of the β-sheets (Figure 1). FEZ-1 may be subdivided into two domains. The N-terminal domain is formed by four short α-helices (α1–α4) and a β-sheet (strands β1–β7) and the second domain by a β-sheet (strands β8–β12) followed by four α-helices (α5–α8) in the C-terminal region. An approximate internal molecular 2-fold symmetry is observed between the two domains, suggesting a possible gene duplication.[8] Structural alignment of L1 with FEZ-1 reveals several differences between the two structures (Figure 2). The major differences are the lack of the L1 N-terminal 3_{10}

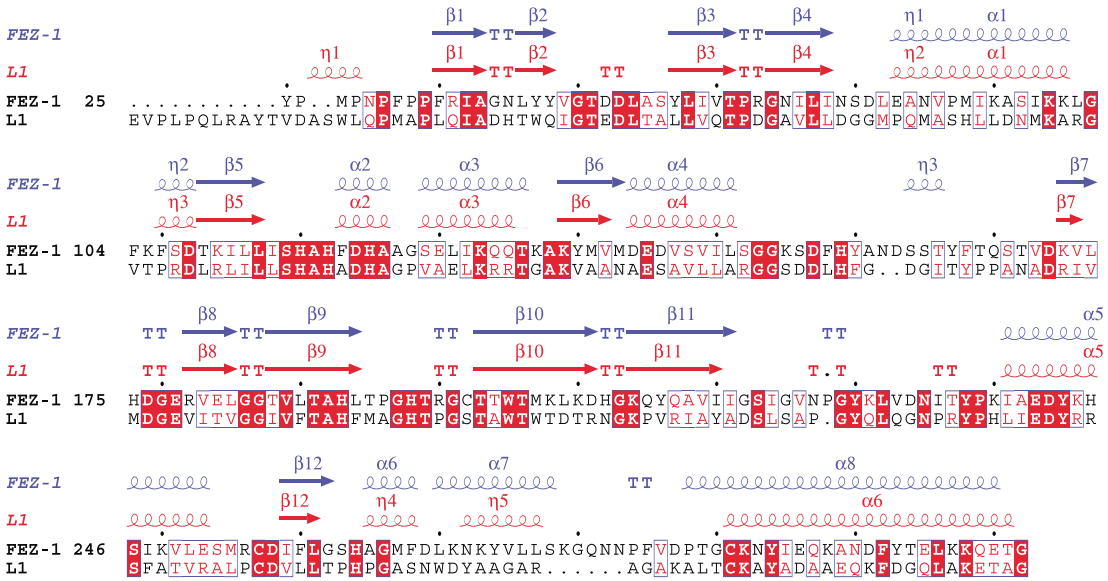

Figure 2. Sequence alignment and secondary structure assignment for FEZ-1 and L1 β-lactamases. Residues that are conserved or similar in the two sequences are shown as red and white boxes, respectively. The Figure was made using ESPript.[29]

helix and the absence of α6 and α7 in L1 where the η5 3_{10} helix is observed (Figure 1). These differences are the result of 13 deletions and six insertions in the L1 sequence. In FEZ-1, there is an additional 3_{10} helix (η3 between α4 and β7, replacing the loop seen in L1. In this region, two residues are inserted into FEZ-1, which enlarge the 155–163 loop near the active site, and displace neighboring residues. Another insertion, Pro226, is also in a loop near the active site. A six residue insertion makes the last α8 helix longer in FEZ-1 than in L1.

There are three cysteine residues in the enzyme, two of which (Cys256 and Cys290) form a disulfide bridge. Cys256 is located in the loop between α5 and β12, and Cys290 is at the N-terminal part of helix α8. This interaction anchors the last long helix (α8) to the rest of the enzyme, stabilizing its position. The third cysteine residue (Cys200) is located immediately before the N-terminal part of β10, in the second β-sheet core and is buried in the structure.

In both native and complexed FEZ-1 there is only one residue in a non-favorable position in the Ramachandran plot. This residue, Asn84, is located immediately after β4 in a buried position. Asn84 is stabilized by different hydrogen bonds between its side-chain and main-chain atoms with residues Ala69, Ser70, Leu113, Ser115 and a water molecule (Wat13, $B = 10$ Å^2). In all subclass B1 and B3 sequences, either aspartic acid or asparagine is found at this position. For all available structures, the equivalent residues have a strained main-chain conformation, supporting the hypothesis of a structural role for the residue. Only one charged amino acid is buried completely in the protein (Asp86). However, this residue is not conserved in all available sequences.

In comparison with subclass B1 β-lactamases, there is a short loop in FEZ-1 between β2 and β3 (corresponding to β3 and β4 in subclass B1). Due to a seven or eight amino acid residue insertion in subclass B1 β-lactamases, the longer loop acts as a flap that closes the active site in the presence of the substrate.[9,15]

Native FEZ-1

Native FEZ-1 presents two molecules per asymmetric unit with an rmsd between chains A and B of 0.09 Å. In each molecule, two Zn ions are located in the active site: Zn1 is in the so-called His-site, being coordinated to His116, His118 and His196; Zn2 is in the second subsite formed by Asp120, His121 and His263 (Table 1). In β-lactamases of subclasses B1 and B2, Cys221 replaces His121 as a Zn ligand in the second site.[10] The two Zn ions are 3.6 Å apart. Close to these ions, a poorly defined electron-density patch was interpreted as being a disordered glycerol molecule from the cryobuffer used for flash-freezing the crystal. This glycerol molecule seems to have displaced the expected bridging hydroxyl ion, placing one of its oxygen atoms (O2) between the two Zn ions. Both Zn1 and Zn2 are coordinated to O2 (2.10 Å and 2.05 Å, respectively) (Table 1). In addition, two different positions were attributed to a disordered water molecule (Wat127 in chain A and Wat178 in chain B). In one position, Wat127/178 is interacting with the Zn ions.

Two residues, Ser221 and Arg255, were found with double conformation: Ser221 presents a double conformation with different occupancies (Figure 3). In its main conformation (occupancy 0.7) the O^{γ} interacts with the above-mentioned disordered water molecule (2.82 Å) when the water

Table 1. Interactions in the active site of native FEZ-1 and FEZ-1-D-captopril (≤3.5 Å)

	Fez-1		Fez-1-D-captopril	
	Atom	Distance (Å)[a]	Atom	Distance (Å)
Zn1	His116 NE2	2.08	His116 NE2	2.16
	His118 ND1	2.08	His118 ND1	2.10
	His196 NE2	2.07	His196 NE2	2.08
	Glycerol[b] O1	2.90	Sulfate O1	2.48
	Glycerol[b] O2	2.10	Sulfate O4	2.60
	Wat127/178	3.28		
Zn2	Asp120 OD1	2.10	Asp120 OD1	2.06
	Asp120 OD2	3.25	Asp120 OD2	3.23
	His121 NE2	2.16	His121 NE2	2.06
	His263 NE2	2.04	His263 NE2	2.04
	Glycerol[b] O2	2.05	Sulfate O1	2.05
	Glycerol[b] O3	2.45		
	Wat 127/178	2.28		

[a] Values for molecule A.
[b] Disordered glycerol molecules with O between Zn atoms.

molecule is further away from the Zn ions. In its main conformation, Ser221 is in contact with ND1 of His196 and the backbone nitrogen atom of Ile222 and Gly223. The secondary conformation (occupancy 0.3) is due to a χ_1 rotation of 103.9°. Upon rotation, the hydroxyl group moves 2.4 Å away from its main position. In this second conformation, Ser221 points towards His116 and Cys200, losing the contact with the water molecule. This molecule is then "liberated" and able to move closer to the Zn ions (Figure 3).

Arg255 is the other residue that presents a double conformation in the native FEZ-1 structure. This residue is exposed to the solvent and located at the contact interface between molecules A and B, which are related by non-crystallographic symmetry.

The FEZ-1 D-captopril complex (FEZ-1 Dcap)

The protein has the same structural features as the native FEZ-1 (rmsd of 0.14 Å and 0.15 Å for molecules A and B, respectively). In the complex, Ser221 and Arg255 show only one conformation. The conformation of Ser221 is identical with that of Ser221 in native FEZ-1, in the conformation with the highest occupancy (0.7), while Arg255 adopts a conformation different from those found in the native enzyme.

The two Zn ions located in the active site of FEZ-1-Dcap make almost identical interactions with the protein ligands as in native FEZ-1 (Table 1). Surprisingly, instead of a glycerol molecule, a sulfate ion from the crystallization buffer was identified close to both Zn atoms, interposing one of its oxygen atoms (O1) between the two ions (2.48 Å to Zn1 and 2.05 Å to Zn2) (Figure 4(a)). The sulfate ion is stabilized in this position by the hydrogen bond between its O4 atom and ND2 of Asn225 (2.71 Å). Zn1 is pentacoordinated to the three His residues of the His-site (NE2 of His116, ND1 of His118 and NE2 of His196) and sulfate O1 and O4 atoms, in a bidentate fashion, and Zn2 is tetracoordinated to OD1 of Asp120, NE2 of His121, NE2 of His263 and sulfate O1 (Table 1).

Initial $2F_o - F_c$ electron density maps showed additional discontinuous density located near the

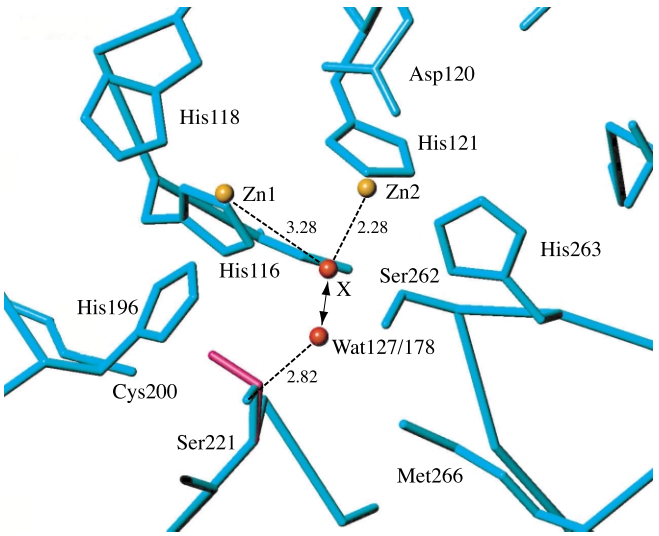

Figure 3. A representation of Ser221 and Wat127/178, close to the active site of native FEZ-1. The alternate conformation of Ser221 with occupancy 0.3 due to a rotation of 103.9° of its hydroxyl group from the main conformation (blue) is depicted in pink. In that main position, Ser221 is hydrogen bonding Wat127/178. In the second conformation, the water is released by Ser221 and attracted close to the Zn ions. The Figure was made using TURBO.

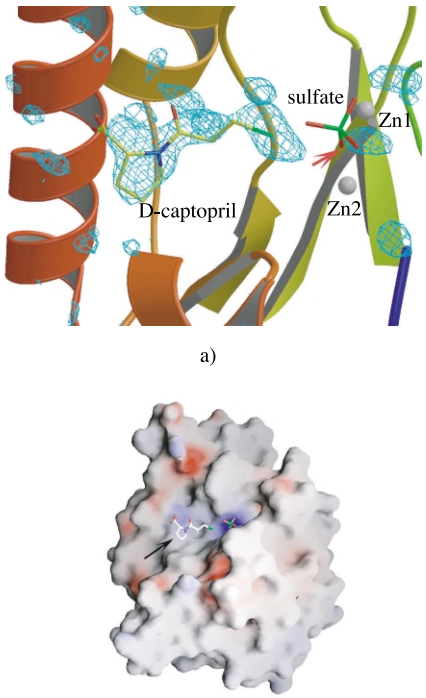

Figure 4. (a) $F_o - F_c$ map contoured at 2.8σ corresponding to the area where the D-captopril was modelled in the structure of FEZ-1-Dcap. The phases were calculated from coordinates not completely refined and without D-captopril. Final refined coordinates have been superimposed. In the proximity, a sulfate ion has one of its oxygen atoms (red arrow) bonded to both Zn ions. The Figure was made with BOBSCRIPT.[30] (b) GRASP representation of FEZ-1-Dcap structure. The D-captopril moiety is located in the positively charged cavity connected to the active site (black arrow). The sulfate ion is depicted. The Figure was made with GRASP (www.csb.yale.edu/userguides/graphics/grasp).

active site. This additional density was confirmed by $F_o - F_c$ maps (Figure 4(a)). Despite discontinuities in the electron density, a molecule of D-captopril 1-(D-3-mercapto-2-methyl-1-oxypropyl)-D-proline; $C_9H_{15}NO_3S$) was fitted and refined, with no clashes or steric problems. The active site of FEZ-1 is located in a wide-open groove, which is mostly positively charged (Figure 4(b)). The modeled molecule of D-captopril completely fills the groove. Due to the observed disorder, an occupancy of 1.0 was assigned to the ring of the D-proline, main-chain atoms and thiol group, and an occupancy of 0.0 for all the other atoms. The closest interaction of the sulfur is with the Ser221 side-chain (2.86 Å).

Discussion

Native FEZ-1

The main differences between native FEZ-1 and FEZ-1-Dcap are concerned with the mobility of certain elements that are related directly with the active site; in particular, the movement of Ser221 and water molecule 127/178 (corresponding to chain A and B of the asymmetric unit) (Figure 3).

In L1, Ser221 has a completely different position than that in any of the two conformations seen in FEZ-1. This is due to a flip of the main-chain in FEZ-1 around the peptide bond of Gly220, which in L1 is aspartic acid. In L1 a neighboring serine residue (Ser223) sterically prevents Ser221 from being in its main conformation. This is not the case in FEZ-1, where Ser223 is replaced by glycine. We conclude that the presence of Gly220 and Gly223 in FEZ-1 allows a greater flexibility in that area, permitting a new orientation of Ser221. In L1 there are two discrete water molecules (Wat10 and Wat85) in positions similar to that of the moving water molecule 127/178 in FEZ-1, but these water molecules make different interactions. In L1, Wat10 adopts a position similar to that of Wat127/178 close to the Zn ions but, in contrast to FEZ-1, it is close to O^{γ} Ser221 (2.72 Å). Wat82 makes four hydrogen bonds: one with O^{γ} Ser223, one with Wat10 and the rest with two water molecules.

Ser221 may play a role in the relay of water molecules from the bulk solvent to the proximity of the active site. By analogy to the model proposed for catalysis in L1,[14] the water molecule would be ready to lose a proton and move to bridging hydroxyl site (Figure 3). It is possible that in our high-resolution structure we observed a water molecule being pushed by Ser221 from the bulk solvent towards the active site, but this water molecule remains mobile due to the presence of the disordered glycerol molecule. The presence of a disordered molecule of glycerol from the cryo-buffer in the active site and the fact that one of its oxygen atoms is located in the position where the activated water molecule should be located, suggests that glycerol acts as a pseudo-inhibitor.

FEZ-1-D-captopril

In the structure of FEZ-1 co-crystallized in the presence of D-captopril, a discontinuous electron density was observed in the proximity of the active site. The clearest section of this electron density coincided with the position of the D-proline ring of the D-captopril molecule, allowing the positioning of a molecule of D-captopril. Its interaction with the enzyme is electrostatically favored by the positively charged groove.

The overall poor electron density for the inhibitor indicates low occupancy and/or a high mobility of certain groups of the molecule. This observation could be explained by the high dissociation constant, K_i, of D-captopril for FEZ-1 (400 μM) compared to that (8 μM) for L1. There is no close interaction between the thiol group of the D-captopril molecule and the two Zn ions of the active site (4.53 Å to Zn1 and 4.30 to Zn2), in contrast to what is observed in a complex between IMP-1 and a mercaptocarboxylate inhibitor,[9]

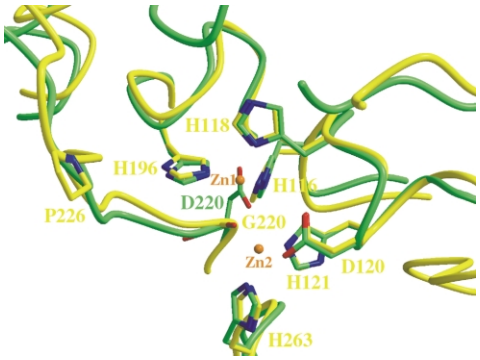

Figure 5. Superposition of the active-site region of FEZ-1 (in yellow) and L1 (in green). For clarity, only side-chain residues listed in the text are represented. Note the insertion of P226 in FEZ-1 and the flip of the main-chain carbonyl oxygen atom in G220 in comparison with D220 in L1. The Figure was made with BOBSCRIPT.

where the sulfur moiety interacts with both Zn atoms.

Additionally, a sulfate molecule within the active site replaces the bridging hydroxide group normally located between the two Zn atoms, since one of its oxygen atoms interacts with both zinc ions, much like in the case of the glycerol group in the native FEZ-1 structure (Table 1). Similar interactions have been described for IMP-1 complexed to a potent succinic acid inhibitor; in this structure, a carboxyl oxygen atom from the inhibitor replaces the bridging water molecule by binding to the zinc atoms.[16] In the present structure, the presence of this intercalated sulfate molecule could preclude a closer interaction of D-captopril with the Zn ions.

Active site of FEZ-1 and L1

The superposition of the two active sites shows significant differences, which can be clustered into three categories. First, the nature of the residue hydrogen bonded to the Zn ligands is different for His116, His118, His196 and His263. For example, in FEZ-1, His116 interacts with O Gly220, whereas the same residue is interacting with OD1 Asp220 in L1 (BBL numbering) (Figure 5). Second, two regions show large deviations (>3 Å) in their backbone positions: the 15 N-terminal residues and the 155–163 loop. Third, small local changes affect the shape of the active site. The main differences are the result of the flipping of the main-chain around the Gly220 peptide bond of and the insertion of Pro226 between β11 and α5 (Figure 5).

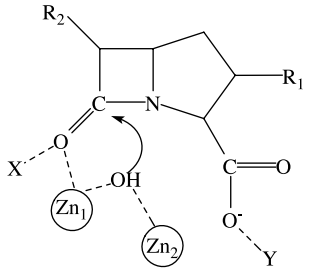

Figure 6. An illustration of the mechanism proposed for carbapenem hydrolysis.

Reaction mechanism

The catalytic mechanism of β-lactam hydrolysis has been proposed to involve the bridging hydroxide group between the two zinc atoms, which can serve as the attacking nucleophile on the carbonyl carbon atom of the β-lactam ring (Figure 6).[14,17,18] In addition, two binding interactions were postulated. First, Asn233 (X in Figure 6) and Zn1 form an oxyanion hole. The side-chain of the equivalent residue in L1 and FEZ-1 is 14 Å away from the postulated oxyanion hole. In L1, Tyr228 was postulated to stabilize the oxyanion, either directly or through a water molecule.[14] In FEZ-1, Tyr228 is conserved. However, Asn225, which is not conserved in L1, is in a better position to play the role of Asn233, which is present in *B. cereus*, *B. fragilis* and IMP-1. Second, a significant contact is formed between the substrate carboxyl group and Ser223 (Y in Figure 6). However, in FEZ-1, Ser223 is mutated into glycine and no other residue could play the same role. A motion of the 223–229 loop upon substrate binding cannot be ruled out, which can bring other side-chain residues to play the role of X and Y. Another possibility is that electrostatic interactions between the negatively charged β-lactam and the positively charged active-site cleft provide the major contribution to binding energy. Interactions of the oxygen carbonyl group and the nitrogen atom of the β-lactam with zinc ions serve to orient the substrate in the active site. The absence of specific protein-substrate interactions thus provides an explanation for the exceptional broad substrate profile of class B β-lactamases.

Tetramerization

FEZ-1 is monomeric in contrast to L1, which is tetrameric (*D2* symmetry). A detailed analysis of the residues involved in the tetramerization of L1 showed that most of these residues are absent or mutated in FEZ-1. In L1, tetramerization is achieved by three defined sets of interactions, allowing each subunit to interact with the other three. The two most striking sets of interactions involve the N terminus region: the first 15 residues make electrostatic and hydrophobic interactions with another subunit (A and B or C and D). FEZ-1 lacks the N terminus region and consequently lacks all of these interactions. The last set of interactions between the A and B subunits is made by the Met175 side-chain, which penetrates into a hydrophobic pocket defined by Leu154, Pro198 and Tyr236. In FEZ-1, these two hydrophobic residues, Met and Pro, are replaced by two positively charged residues, His175 and Arg198, respectively

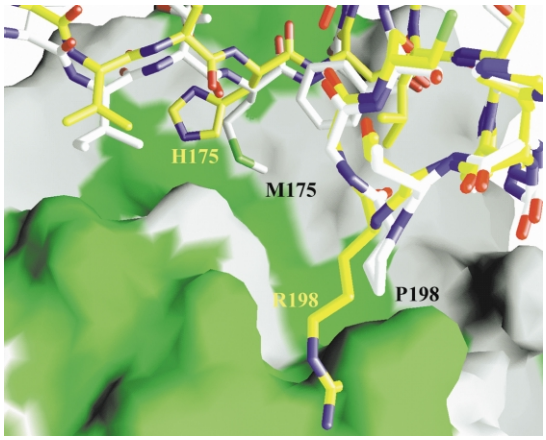

Figure 7. GRASP representation of the main zone of interactions between monomers A and B in tetramer L1. Subunit A of L1 is depicted as a chain with white carbon atoms. A superposition of the structurally related area of FEZ-1 is depicted in yellow. For clarity, only residues from 171 to 200 are represented. Monomer B is depicted as a surface where the green area corresponds to the localization of hydrophobic residues.

(Figure 7). These two mutations prevent interactions between subunits.

Packing

The packing arrangement of the protein molecules into the two crystal forms is very similar. One unit cell can be converted to the other by permutation of the *a* and *c* axes. The C2 form is transformed into the $P2_1$ form by an origin translation (1/4,0,0) from a 2 axis to a 2_1 axis. The 2 axis of *C*2, after a slight translation in the plane (*a*,*c*), is the non-crystallographic 2-fold rotation axis between molecules A and B, in $P2_1$.

Conclusions

Zn-β-lactamases are members of a superfamily that includes proteins with a large variety of biological functions.[19] As well as class B β-lactamases, the superfamily includes glyoxalases II, arylsulfatase, flavoproteins, cyclase/dehydrase and RNA 3′ processing protein; the occurrence of these proteins spans from bacterial to human species.

The two structures presented here contribute to unravel the structure/function relationships of an important class of enzymes involved in drug resistance. Ultimately, a full understanding of the catalytic mechanism may be important in the development of urgently needed inhibitors.

Materials and Methods

Overexpression and purification

The overexpression and purification of FEZ-1 was performed as described.[12] FEZ-1 is a monomeric enzyme of 263 residues; the molecular mass (29,332 Da) was confirmed by electrospray mass-spectrometry before crystallographic analysis.

Synthesis of D-captopril

D-captopril (1-(D-3-mercapto-2-methyl-1-oxypropyl)-D-proline; $C_9H_{15}NO_3S$) was synthesized from commercially available compounds starting with D-proline.[20,21] The final hydrolysis reaction was carried out with 1 M NaOH under an argon atmosphere.

Crystallization

Native crystals of dimensions 450 μm × 80 μm × 40 μm were obtained after approximately ten days by hanging-drop, vapor-diffusion at 20 °C. A sample (1 μl) of protein solution (10.5 mg per ml of 15 mM sodium cacodylate/cacodylic acid, pH 6.0) was mixed with 1 μl of 20% (w/v) PEG 4000, 0.2 M ammonium sulfate, 20 μM $ZnCl_2$, 0.1 M sodium acetate/acetic acid (pH 5.0) as a precipitant solution. The crystals belong to the space group $P2_1$ with unit cell parameters $a = 44.86$ Å, $b = 76.85$ Å, $c = 78.89$ Å and $\beta = 102.08°$, and contain two molecules per asymmetric unit (Table 2).

Co-crystallization with D-captopril was set up by mixing in the crystallization drops 1 μl of the protein solution, 1 μl of 18% PEG MME 5000, 0.2 M ammonium sulfate, 0.1 M Hepes pH 7.0, 0.25 μl of 0.1 mM $ZnCl_2$ and 0.3 μl of 36 mM D-captopril. Crystals started appearing after ten days. The crystal chosen for data collection measured approximately 350 μm × 50 μm × 20 μm and was also monoclinic, but belonged to the space group *C*2 with unit cell dimensions $a = 82.12$ Å, $b = 76.78$ Å, $c = 44.84$ Å and $\beta = 110.201°$, with one molecule per asymmetric unit (Table 2).

Data collection

X-ray data from a crystal obtained by co-crystallization with D-captopril at 8 °C were collected in house using a Nonius FR 591 rotating anode X-ray generator running at 40 kV and 100 mA, coupled to a Mar Research Imaging Plate detector. Diffraction data to 1.78 Å resolution were obtained from the crystal flash-cooled directly in the cryostream after soaking for a few minutes in cryoprotectant solution (same crystallization conditions with additional 20% glycerol).

A native FEZ-1 crystal was analyzed on the BM30A X-ray beam-line at the European Synchrotron Radiation Facility (ESRF) in Grenoble. In order to prepare the protein-inhibitor complex, the native crystal was presoaked for 15 minutes with 14.4 μM D-captopril freshly added to the reservoir solution. The crystal was transferred to a cryoprotectant solution for a few minutes (same crystallization conditions with 25% added glycerol) and then flash-cooled directly in the cryostream. A data set collection of 180 frames using 1° oscillation steps to 1.65 Å resolution was collected at a wavelength of $\lambda = 0.9$ Å.

Due to the expected presence of two Zn atoms in the active site, a crystal obtained from co-crystallization with D-captopril at 20 °C was used on the same beamline for a SAD experiment to detect the Zn atoms positions. The flash-cooling procedure described above was applied to a crystal. Data collection was performed at a wavelength of $\lambda = 1.2827$ Å previously determined from a fluorescence spectrum on the same crystal, which

Table 2. X-ray data collection and structure refinement

	FEZ-1	FEZ-1-D-captopril	
A. *Data collection statistics*			
		I[a]	II[b]
Unit cell parameters			
a (Å)	44.86	82.12	83.07
b (Å)	76.85	76.78	76.90
c (Å)	78.89	44.84	44.92
β (deg.)	102.08	110.2	109.81
Space group	$P2_1$	*C*2	*C*2
Molecules/asymmetric unit	2	1	1
Max. resolution (Å)	1.65	1.78	2.35
No. observed reflections	217,456	74,560	68,707
No. unique reflections	61,458	46,214	21,850
Overall completeness (%)	97.9 (96.9)[c]	92.4 (61)[d]	98.4 (96.4)[e]
Multiplicity	3.5	3.2	6.3
R_{sym}[f]	0.021 (0.037)[c]	0.038 (0.076)[d]	0.054 (0.065)[e]
B. *Refinement statistics*			
No. reflections	61,308	45,143	
No. atoms (non-H)	4452	2321	
$R_{working}$[g] (%)	17.37	16.78	
R_{free}[h] (%)	19.83	19.10	
rms deviation from ideal			
Bonds (Å)	0.014	0.014	
Angles (deg.)	1.62	1.59	

[a] Data collection in laboratory X-ray generator.
[b] Data collection from synchrotron source.
[c] Last resolution shell 1.74–1.65 Å.
[d] Last resolution shell 1.88–1.78 Å.
[e] Last resolution shell 2.48–2.35 Å.
[f] $R_{sym} = \sum|I_j - \langle I\rangle|/\sum\langle I\rangle$, where I_j is the intensity for reflection j, and $\langle I\rangle$ is the mean intensity.
[g] $R_{working} = \sum||F_o| - |F_c||/\sum|F_c|$, calculated with the working set.
[h] R_{free} was similarly calculated with approximately 10% of the data excluded from the calculation of $R_{working}$.

corresponds to the energy of Zn K absorption edge. The maximum resolution of the data collection was 2.35 Å. All data sets were processed and scaled with DENZO[22]and SCALA[23] (Table 2).

Structure determination and refinement

The structure of FEZ-1 co-crystallized with D-captopril was solved using molecular replacement with the program AmoRe.[24] One monomer of the L1 subclass B3 β-lactamase was used as a search model (PDB ID 1SML) after removing the N-terminal 13 residues, Zn ions, hetero atoms and water molecules. Reflections between 15 Å and 4.0 Å were included in the molecular replacement calculations. The best solution obtained has a correlation factor of 22.7% and an *R*-factor of 50.0%. Rigid-body calculation using CNS[25] and further analysis of an initial density map by the interactive graphics program TURBO† confirmed the solution to be correct. The initial search model was then converted into a poly-alanine chain. To improve the model, rounds of model building and iterative simulated annealing using torsion angle dynamics (starting temperature 5000 K with cooling rate 50 K per cycle), energy minimization and *B*-factor refinement using CNS tasks, were performed. At this point the model still had ambiguous zones ($R_{working}$ 36.9%; R_{free} 44.2%; with approximately 10% of reflections in the test set for cross-validation).

A SAD experiment was made using the crystal obtained in co-crystallization with D-captopril. Diffraction data were collected at the anomalous edge of Zn. The two expected Zn sites were identified in the asymmetric unit simultaneously by using the program Shake-and-Bake[26] and visually by straight calculation of an anomalous Patterson map from a script of the CCP4 suite.[23] These positions were refined by MLPHARE[23] with an overall figure of merit (FOM) from 0.271 Å to 2.34 Å. The phases were further improved by density modification using DM,[23] giving an FOM of 0.654.

Phase information from the SAD experiment was included at that point for further refinement of the partially built model obtained by molecular replacement. Experimental phases (experimental Hendrickson–Lattman coefficients) were calculated with the program CNS and incorporated into the refinement of the partially built model. Initial refinement was started by simulated annealing (torsion angle dynamics with starting $T = 5000$ K and a cooling rate of 50 K per cycle) followed by successive rounds of model building, energy minimization and B-factor refinement. Phase information helped to improve the previously built model and to solve the ambiguities found initially.

When the model was considered to be correct, 263 water molecules were added automatically (CNS). In the last steps of refinement, four sulfate ions and one chloride ion were incorporated. One sulfate ion was fitted close to the Zn ions. In addition, a molecule of D-captopril was modeled and refined to fit the extra electronic density found in the active site. Even if the inhibitor was not exhibiting full occupancy, it could be positioned with no electrostatic or steric disagreements. Topology and parameters files of the hetero-compounds were generated using the program XPLO2D included in

† www.csb.yale.edu/userguides/graphics/turbofrodo

the HIC-UP server†. The final structure FEZ-1-D-captopril has $R_{working} = 16.8\%$ and $R_{free} = 19.1\%$ (Table 2).

The native structure of FEZ-1 at 1.65 Å was solved by molecular replacement using the program AMoRe. The previous structure of FEZ-1 without solvent and Zn ions was used as a search model. A solution corresponding to two molecules per asymmetric unit was obtained with a correlation coefficient of 73.4% and an *R*-factor of 34.7%. Non-crystallographic symmetry matrices that relate the two models in the asymmetric unit were calculated using CNS. Non-crystallographic symmetry restraints were applied during all refinement procedures. Iterative rounds of model building, energy minimization and *B*-factor refinement followed. The restraint weight applied in the non-crystallographic symmetry was initially 300 kcal mol^{-1} $Å^{-2}$ and decreased progressively in the last refinement procedures to 20. In the final model, 540 water molecules, four sulfate ions, three acetate ions, and four molecules of glycerol were added. One of the glycerol molecules in two different conformations was placed in the active site of each of the two molecules in the asymmetric unit (A and B) to interpret the highly disordered electronic density found in that area. Double conformations were included in the last steps of refinement for the residues Ser221 and Arg 255 in chains A and B of the asymmetric unit and double position for water molecules 127 and 178, which are disordered water molecules in the active sites of the two chains. The final model had $R_{working} = 17.4\%$, and $R_{free} = 19.8\%$ (Table 2). The quality of the two structures was analyzed by PROCHECK.[27]

Protein Data Bank coordinates

The atomic coordinates have been deposited in the Protein Data Bank (PDB). The PDB ID code for the native FEZ-1 structure is 1K07 and that for the FEZ-1 D-captopril complex is 1JT1.

Acknowledgements

We acknowledge assistance by the beamline staff of BM30, European Synchrotron Research Facility, Grenoble, France. An ECC grant Human and Mobility no. ERB-FMRX-CT98-0232 and PAI P5/33 from the Belgian government supported this work.

References

1. Rasmussen, B. A. & Bush, K. (1997). Carbapenem-hydrolyzing beta-lactamases. *Antimicrob. Agents Chemother.* **41**, 223–232.
2. Arakawa, Y., Murakami, M., Suzuki, K., Ito, H., Wacharotayankun, R., Ohsuka, S. *et al.* (1995). A novel integron-like element carrying the metallo-beta-lactamase gene blaIMP. *Antimicrob. Agents Chemother.* **39**, 1612–1615.
3. Lauretti, L., Riccio, M. L., Mazzariol, A., Cornaglia, G., Amicosante, G., Fontana, R. & Rossolini, G. M. (1999). Cloning and characterization of blaVIM, a new integron-borne metallo-beta-lactamase gene from a *Pseudomonas aeruginosa* clinical isolate. *Antimicrob. Agents Chemother.* **43**, 1584–1590.
4. Bush, K. (1999). Beta-Lactamases of increasing clinical importance. *Curr. Pharm. Des.* **5**, 839–845.
5. Rasia, R. M. & Vila, A. J. (2002). Exploring the role and the binding affinity of a second zinc equivalent in *Bacillus cereus* metallo-beta-lactamase. *Biochemistry*, **41**, 1853–1860.
6. Wommer, S., Rival, S., Heinz, U., Galleni, M., Frère, J. M., Franceschini, N. *et al.* (2002). Substrate-activated zinc binding of metallo-beta-lactamases: physiological importance of the mononuclear enzymes. *J. Biol. Chem.*, **277**, 24142–24147.
7. Wang, Z., Fast, W. & Benkovic, S. J. (1999). On the mechanism of the metallo-beta-lactamase from *Bacteroides fragilis*. *Biochemistry*, **38**, 10013–10023.
8. Carfi, A., Parès, S., Duée, E., Galleni, M., Duez, C., Frère, J. M. & Dideberg, O. (1995). The 3-D structure of a zinc metallo-beta-lactamase from *Bacillus cereus* reveals a new type of protein fold. *EMBO J.* **14**, 4914–4921.
9. Concha, N. O., Janson, C. A., Rowling, P., Pearson, S., Cheever, C. A., Clarke, B. P. *et al.* (2000). Crystal structure of the IMP-1 metallo beta-lactamase from *Pseudomonas aeruginosa* and its complex with a mercaptocarboxylate inhibitor: binding determinants of a potent, broad-spectrum inhibitor. *Biochemistry*, **39**, 4288–4298.
10. Galleni, M., Lamotte-Brasseur, J., Rossolini, G. M., Spencer, J., Dideberg, O. & Frere, J. M. (2001). Standard numbering scheme for class B beta-lactamases. *Antimicrob. Agents Chemother.* **45**, 660–663.
11. Boschi, L., Mercuri, P. S., Riccio, M. L., Amicosante, G., Galleni, M., Frere, J. M. & Rossolini, G. M. (2000). The legionella *Fluoribacter gormanii* metallo-beta-lactamase: a new member of the highly divergent lineage of molecular-subclass B3 beta-lactamases. *Antimicrob. Agents Chemother.* **44**, 1538–1543.
12. Mercuri, P. S., Bouillenne, F., Boschi, L., Lamotte-Brasseur, J., Amicosante, G., Devreese, B. *et al.* (2001). Biochemical characterization of the FEZ-1 metallo-beta-lactamase of *Legionella gormanii* ATCC 33297(T) produced in *Escherichia coli*. *Antimicrob. Agents Chemother.* **45**, 1254–1262.
13. Simm, A. M., Higgins, C. S., Pullan, S. T., Avison, M. B., Niumsup, P., Erdozain, O. *et al.* (2001). A novel metallo-beta-lactamase,Mbl1b, produced by the environmental bacterium *Caulobacter crescentus*. *FEBS Letters*, **509**, 350–354.
14. Ullah, J. H., Walsh, T. R., Taylor, I. A., Emery, D. C., Verma, C. S., Gamblin, S. J. & Spencer, J. (1998). The crystal structure of the L1 Metallo-beta-lactamase from *Stenotrophomonas maltophilia* at 1.7 Å resolution. *J. Mol. Biol.* **284**, 125–136.
15. Fitzgerald, P. M. D., Wu, J. K. & Toney, J. H. (1998). Unanticipated inhibition of the metallo-beta-lactamase from *Bacteroides fragilis* by 4-morpholineethanesulfonic acid (MES): a crystallographic study at 1.85-Å resolution. *Biochemistry*, **37**, 6791–6800.
16. Toney, J. H., Hammond, G. G., Fitzgerald, P. M., Sharma, N., Balkovec, J. M., Rouen, G. P. *et al.* (2001). Succinic acids as potent inhibitors of plasmid-borne imp-1 metallo-beta-lactamase. *J. Biol. Chem.* **276**, 31913–31918.
17. Concha, N. O., Rasmussen, B. A., Bush, K. & Herzberg, O. (1996). Crystal structure of the wide-spectrum binuclear zinc β-lactamase from *Bacteroides fragilis*. *Structure*, **4**, 823–836.

† http://xray.bmc.uu.se/hicup/

18. Wang, Z., Fast, W., Valentine, A. M. & Benkovic, S. J. (1999). Metallo-beta-lactamase: structure and mechanism. *Curr. Opin. Chem. Biol.* **3**, 614–622.
19. Daiyasu, H., Osaka, K., Ishino, Y. & Toh, H. (2001). Expansion of the zinc metallo-hydrolase family of the beta-lactamase fold. *FEBS Letters*, **503**, 1–6.
20. Suh, J. T., Skiles, J. W., Williams, B. E., Youssefyeh, R. D., Jones, H., Loev, B. *et al.* (1985). Angiotensin-converting enzyme-inhibitors-new orally active antihypertensive (mercaptoalkanoyl)-glycine and [(acylthio)alkanoyl] glycine derivatives. *J. Med. Chem.* **28**, 57–66.
21. Skiles, J. W., Suh, J. T., Williams, B. E., Menard, P. R., Barton, J. N., Loev, B. *et al.* (1986). Angiotensin-converting enzyme-inhibitors-new orally active 1,4-thiazepine-2,5-diones, 1,4-thiazine-2,5-diones, and 1,4-benzothiazepine-2,5-diones possessing antihypertensive activity. *J. Med. Chem.* **29**, 784–796.
22. Otwinowski, Z. & Minor, W. (1997). Processing of X-ray diffraction data collected in oscillation mode. *Methods Enzymol.* **276**, 307–326.
23. Collaborative Computational Project Number 4 (1994). The CCP4 suite: programs for protein crystallography. *Acta Crystallog. sect. D*, **50**, 760–763.
24. Navaza, J. (1994). AMoRe: an automated package for molecular replacement. *Acta Crystallog. sect. A*, **50**, 157–163.
25. Brünger, A. T., Adams, P. D., Clore, G. M., DeLano, W. L., Gros, P., Grosse-Kunstleve, R. W. *et al.* (1998). Crystallography & NMR system: a new software suite for macromolecular structure determination. *Acta Crystallog. sect. D*, **54**, 905–921.
26. Miller, R., Gallo, S. M., Khalak, H. G. & Weeks, C. M. (1994). SnB: crystal structure determination via Shake-and-Bake. *J. Appl. Crystallog.* **27**, 613–662.
27. Laskowski, R. A., MacArthur, M. W., Moss, D. S. & Thornton, J. M. (1993). PROCHECK: a program to check the stereochemical quality of protein structures. *J. Appl. Crystallog.* **26**, 283–291.
28. Kraulis, P. J. (1991). MOLSCRIPT: a program to produce both detailed and schematic plots of protein structures. *J. Appl. Crystallog.* **24**, 946–950.
29. Gouet, P., Courcelle, E., Stuart, D. I. & Metoz, F. (1999). ESPript: analysis of multiple sequence alignments in PostScript. *Bioinformatics*, **15**, 305–308.
30. Esnouf, R. M. (1999). Further additions to MolScript version 1.4, including reading and contouring of electron-density maps. *Acta Crystallog. sect. D*, **55**, 938–940.

Edited by R. Huber

(Received 8 July 2002; received in revised form 25 October 2002; accepted 28 October 2002)